International Journal of Engineering and Technical Research (IJETR)
ISSN: 2321-0869 (O) 2454-4698 (P) Volume-8, Issue-4, April 2018

Bending- Compressing Characteristics and ABAQUS Simulation of Soil Based Caragana Reinforced Materials

Wang Sheng, Guo Yuming

Abstract— **The stress of reinforced material soil based Caragana under compression and bending deformation is observed through experiments. The finite element numerical simulation of these two properties is carried out through ABAQUS software, obtaining the stress and strain fields of the material under two basic deformation. Compared with the results of the test and ABAQUS numerical simulation, the error is very small, which shows that the ABAQUS modeling can simulate the stress and deformation process of the materials well.**

Index Terms— **Caragana; soil base; numerical simulation; compressing-bending characteristics**

I. INTRODUCTION

As a crop widely planted in Northern China, Caragana has played a very important role in the process of building the environment friendly society because of its advantages of cold tolerance, drought, drought, and high survival rate [1]. After studying the biomechanical properties and dynamic indexes of Caragana raw material, fiber and solid material, it was found that its tensile strength, compared with the straw or other sandy shrubs [2], such as Salix, willow and poplar, was higher [3]. Taking advantage of the excellent mechanical properties of Caragana, the traditional soil materials are optimized and studied [4].

At present, the finite element models of composite materials mainly have three forms: integral, separated and combined [5]. In the integral finite element model, the composite material is dispersed in the whole cell, and it is regarded as continuous uniform material [6]. If the contribution of a material to the whole material is enhanced, the mechanical parameters of the material can be adjusted, such as the increase of the yield strength and the modulus of elasticity of the material [7,8]. The obvious shortcoming of the integral model is that the parameters in the simulation are based on the experimental data. Due to the measurement error, the calculation results will be deviant from the engineering practice, and the micro mechanism of strengthening the interaction between the material and the soil cannot be revealed [9].

In the separated model, the reinforced material and soil are divided into small enough units, and a variety of different unit forms are chosen according to the different mechanical properties of the soil and the reinforced material [10]. The reinforced material is one-dimensional bar unit and the soil body is beam entity unit. However, this model does not consider the possible slippage and embeddedness between reinforcement materials. The combined analysis model is between the integral and separated models [11]. In fact, after being subjected to external forces, the relative slippage between the two materials will occur. In this model, the plane element is used to connect the interfaces between the units.

Wang Sheng, (1991 -), male, graduate student, School of engineering,Shanxi Agricultural University, Taigu, 030801, China
Guo Yuming, (1954 -), male, Shanxi pacification, Professor, doctoral supervisor

II. TEST PROCESS

2.1 Test materials and equipment

This experiment is an extended study of a series of experiments. Its Test materials and equipment, preparation and test method of sample can refer to the author's paper published in this magazine [12]. Figure 1 is the test device for the specimen.

Fig. 1 is the bending and compression test device for the specimen

2.2 Test result

For the compression specimen, the maximum stress represented by the stress strain curve is the strength limit. The calculation formula is

$$\sigma = \frac{F}{S} \qquad (1)$$

σ is stress, MPa; F is force, N; S is cross section area, mm^2

For rectangular bending specimens, the maximum normal stress at the mid span section is calculated according to formula 2.

$$f_{cr} = \frac{3F_{cr}L}{2bh^2} \quad (2)$$

F_{cr} is the maximum load measured in the bending test, N; L is the span of the specimen, mm; b , h the width and height of the specimen respectively, mm.

The arithmetic mean values of repeated samples were obtained by Excel software. The results are summarized as Table1:

Table 1 Test results of basic mechanical properties of soil reinforced by Caragana

Reinforcement length of Caragana	Reinforcement ratio of Caragana /%	Ultimate bending strength /Mpa	Ultimate compressive strength /MPa
0mm	0.00	2041	2.76
<0.16mm	0.05	2200	2.80
<0.16mm	0.10	2338	2.89
<0.16mm	0.15	2379	3.00
<0.16mm	0.20	2471	3.30
<0.16mm	0.25	2560	3.57
<0.16mm	0.30	2473	3.21
0.16~0.63mm	0.05	2603	3.24
0.16~0.63mm	0.10	2705	3.62
0.16~0.63mm	0.15	2762	3.54
0.16~0.63mm	0.20	2885	4.35
0.16~0.63mm	0.25	2942	4.28
0.16~0.63mm	0.30	2674	4.02
0.63~1.25mm	0.05	2799	4.38
0.63~1.25mm	0.10	2991	4.83
0.63~1.25mm	0.15	3188	4.69
0.63~1.25mm	0.20	3296	5.12
0.63~1.25mm	0.25	3102	5.39
0.63~1.25mm	0.30	3354	5.27
1.25~2mm	0.05	3639	4.37
1.25~2mm	0.10	3803	4.83
1.25~2mm	0.15	3925	4.99
1.25~2mm	0.20	4050	5.36
1.25~2mm	0.25	4152	5.47
1.25~2mm	0.30	3913	5.14
2~4mm	0.05	4152	5.27
2~4mm	0.10	4457	5.36
2~4mm	0.15	4570	5.77
2~4mm	0.20	4745	5.42
2~4mm	0.25	4905	5.58
2~4mm	0.30	4705	5.32
4~4.75mm	0.05	4673	5.63
4~4.75mm	0.10	4953	5.72
4~4.75mm	0.15	5249	5.93
4~4.75mm	0.20	5505	6.32
4~4.75mm	0.25	5755	6.15
4~4.75mm	0.30	5370	6.29

III. CALCULATION AND ANALYSIS

In order to verify the correctness and rationality of the test results, ABAQUS6.14 was used to calculate and analyze all the test results.

Material density is $1.530*10^{-3}$g/mm³ , Modulus of elasticity is 54.99MPa , Poisson's ratio is 0.25. The key points of the stress-strain curves obtained from the test are also obtained, as shown in Table 2:

Table2 Stress and strain data of soil based Caragana reinforced materials

ε (10^{-2})	0	1.45	2.56	3.03	3.74	4.32	4.62	4.95	5.08
σ(MPa)	0	1.32	1.67	2.09	2.38	2.5	2.47	2.37	2.15

The initial yield stress, the ultimate stress, the strain corresponding to the ultimate stress, the yield stress and the limit stress ratio were all measured by the test. The displacement pressure of 10mm is applied at a constant speed. In the software analysis step, open the geometric nonlinearity; increase the maximum iteration number IA to 15.

IV. COMPARISON BETWEEN CALCULATION RESULTS AND TEST

4.1 Stress distribution verification

For the simply supported beam in the middle of the specimen, the stress at the two ends of the beam is zero, and the force in the middle is the largest. It can be seen from the figure 2 that the distribution law of stress is basically the same as theory. The force of the specimen in the middle is the largest, and the two sides of the specimen, especially the upper part, are almost zero.

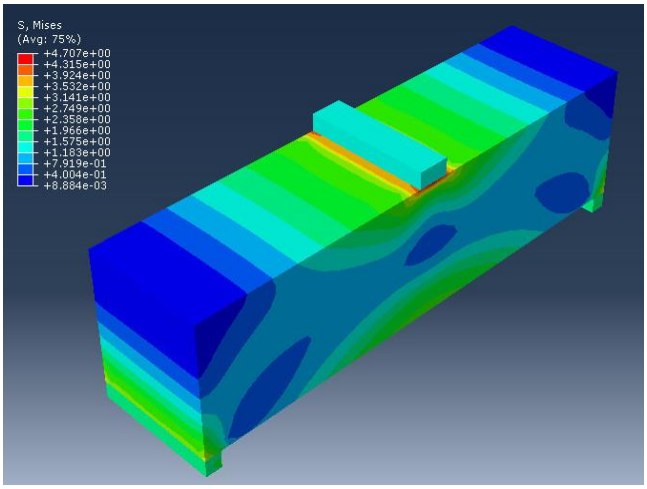

Fig. 2 Material stress cloud chart under the limit of bending of material

According to the knowledge of mechanics of materials, the formula for calculating the normal stress at any point on the cross section of a pure bent beam is:

$$\sigma = \frac{M}{Iz} y \quad (3)$$

In the formula 3, M is the bending moment on the cross section; Iz is the moment of inertia of the section to the neutral axis; y is the distance from the point of stress to the neutral axis.

It is known from the formula 3 that the normal stress is directly proportional to M and y, inversely proportional to Iz. That is, normal stress is linearly distributed along the height of the section, and the farther it is from the center axis, the greater the normal stress. The normal stress on the center axis is zero. For symmetric structures, the magnitude of tensile stress on the midspan section is equal. These laws are also consistent with the distribution law of cloud pictures as figure 2.

Under the condition of ultimate load, the compression stress cloud diagram of test block is shown in figure 3. The stress at both ends of the specimen is obviously larger than that in the middle. In the process of approaching the limit load, the specimen gradually presents an obvious drum shape.

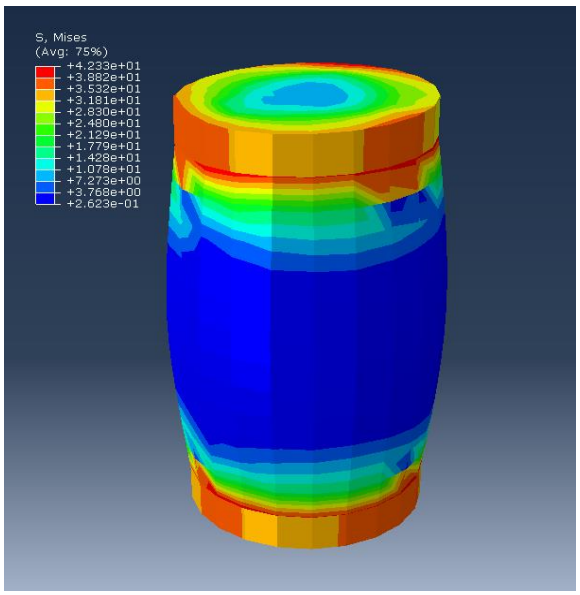

Fig. 3 The cloud picture at the pressure of the specimen

4.2 Verification of principal stress

Using the plug-in extremum to extract the maximum values of each frame. For the bending strength, we can get the curves shown in the figure 4:

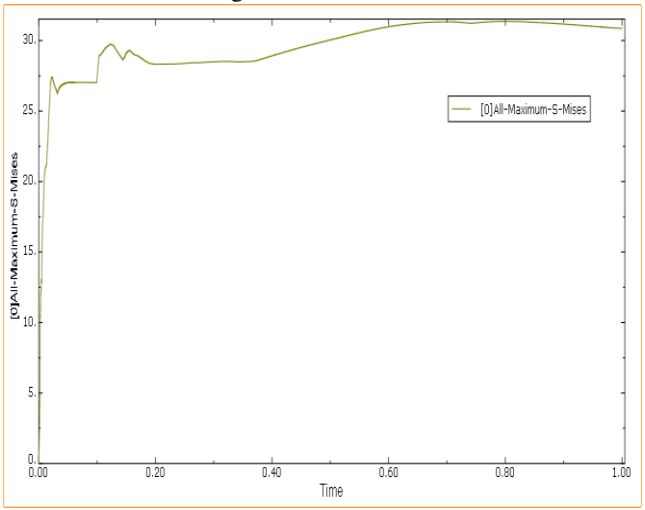

Fig.4 The variation of the stress extremum of the bending specimen with time

For the bending specimen, the maximum stress in the graph is 3323r.86KPa. Whereas, from the above test, we can know that the maximum value of the test data is 5755KPa, and the error is $\frac{5755-3323}{5777}=0.42098$. Within the acceptable range, the results are considered to be effective.

For the compressive strength, we can get the curves shown in the figure 5:

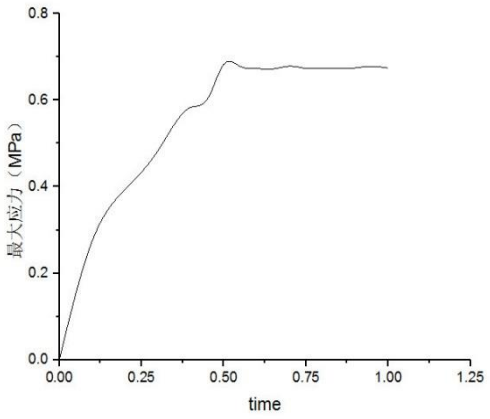

Fig.5 The variation of the compressive strength of specimens with time

Under the compression condition, figure 5 shows that the ultimate stress of the material is 6.829MPa during compression. The test data shows that the limit stress of the optimum ratio of materials corresponding to the reinforcement 4~4.75mm, and Caragana quality 0.25% is 6.15MPa. And the both results are similar, and the error is 11.04%.

4.3 Verification of support counterforce

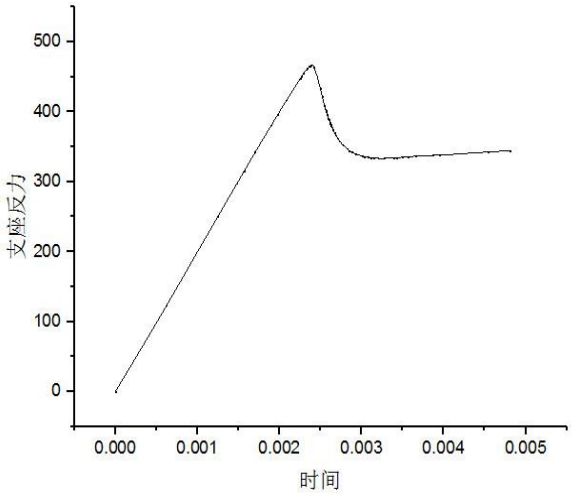

Fig.6 Change of counterforce with time

It can be seen from the figure 6 that the counterforce of the limit is 467N, and the limit reaction force of the test which can be found in 2.2 is 387N. The error of the test is

$$\frac{467-387}{387}=0.206718$$

.

V. CONCLUSION

Based on the foregoing series of studies, the ABAQUS program is used to further explore the bending mechanical properties of soil based Caragana reinforced materials, which have proved is feasible and efficient. The main achievements of this paper are as follows:

(1). The damage model and related parameters of the material are obtained. Finite element static elastoplastic analysis of the stress distribution of soil based Caragana reinforced materials under compression and bending is carried out by using Abaqus.

(2). The comparison of comparison between simulation and test results shows that the ultimate bearing capacity is similar to the test results, and the trend of stress strain curve is in good agreement with the test. The distribution of stress in the damage process is observed by the damage cloud map, and the results can be anastomosed to the test results well.

(3) The calculation, greatly reducing the cost, can provide efficient and reliable engineering practical technical parameters for the related material research.

ACKNOWLEDGEMENTS

Funding for this research was provided by the Special Research Found for the Doctoral Program of Higher Education(20111403130001) and Shanxi Key Laboratory Foundation Project（2013011066-9）.

REFERENCE

[1] Liu Y, He L, An L, et al. Arbuscular mycorrhizal dynamics in a chronosequence of Caragana korshinskii plantations[J]. Fems Microbiology Ecology, 2009, 67(1):81-92.

[2] Gao Z. Study on the Technology of Fiber and Particle Board of Sandy Shrubs[J]. Journal of Neimenggu Forestry College, 1998.

[3] Zhen A N, Tian J F. Study on the Effect of the Front Angle and Cutting Output of Cutting Tools on Caragana Cutting Force[J]. Forestry Machinery & Woodworking Equipment, 2010.

[4] Liang Y, Tao C, Zhou B, et al. Submicron structure random field on granular soil material with retinex algorithm optimization[C]// 2017:12013.

[5] Ling D, Yang Q, Cox B. An augmented finite element method for modeling arbitrary discontinuities in composite materials[J]. International Journal of Fracture, 2009, 156(1):53-73.

[6] Zhou M H, Xiao-Qian L I, Wei J. 3D J-Integral Finite Element Model of Inner Surface Cracks in a Certain Gun Barrel Based on MARC[J]. Journal of Gun Launch & Control, 2010.

[7] Hans-Georg Willschütz, Altstadt E. Development of an Integral Finite Element Model for the Simulation of Scaled Core-Meltdown-Experiments[J]. Forschungszentrum Rossendorf, 2010.

[8] Faraji S, Ting J M, Crovo D S, et al. Nonlinear Analysis of Integral Bridges: Finite-Element Model[J]. Journal of Geotechnical & Geoenvironmental Engineering, 2001, 127(5):454-461.

[9] Sin S J, Hong J H, Sin B C, et al. p-Version Finite Element Model Based on Equivalent Domain Integral Method for 2-D Cracked Panels[J]. 1997.

[10] Karlon W J, Eisenberg S R, Lehr J L. Effects of paddle placement and size on defibrillation current distribution: a three-dimensional finite element model[J]. IEEE transactions on bio-medical engineering, 1993, 40(3):246.

[11]Koolstra J H, van Eijden T M. Combined finite-element and rigid-body analysis of human jaw joint dynamics[J]. Journal of Biomechanics, 2005, 38(12):2431.

[12] Wang S, Guo Y M, Dou J X. Experimental study on mechanical properties and proportioning process optimization of the strengthening material Clay reinforced by Caragana[J] ,International Journal of Engineering and Technical Research (IJETR), 2017, 7(9)：1-5.